Multiple-view camera calibration for large scenes with limited spatial access at the Rotterdam Zoo

Muller, Koen; Tam, Daniel; Westerweel, Jerry

Publication date
2018

Document Version
Final published version

Published in
Proceedings of the 19th International Symposium on Application of Laser and Imaging Techniques to Fluid Mechanics

Multiple-View Camera Calibration for Large Scenes with Limited Spatial Access at the Rotterdam Zoo

K. Muller[1,*], D.S.W. Tam[1], J. Westerweel[1]
1: Laboratory for Aero and Hydrodynamics, Faculty of Mechanical, Maritime and Materials Engineering, Delft University of Technology
* Correspondent author: K.Muller@tudelft.nl

Keywords: Large-scale Camera Calibration, Computer Vision, Field Experiments, Biological Fluid Mechanics

ABSTRACT

Obtaining accurate experimental data from Lagrangian tracking and tomographic velocimetry requires an accurate and consistent camera calibration over multiple views. At length-scales that span beyond the laboratory environment obtaining a camera calibration can be challenging. Combining tools developed in computer vision and non-linear camera mappings known from experimental fluid mechanics, we successfully calibrate a four-camera setup at the large-scale ocean aquarium of the Rotterdam Zoo. The method is valid for any number of cameras and allows retrieving the intrinsic and extrinsic camera properties that can be used to compute the (virtual-)camera positioning and further quality assessment. Using our method we obtain an accurate and consistent camera calibration at large-scale over a space that has limited access.

1. Introduction

Over the past decade, quantitative imaging of large-scale field experiments has gained new application to both biophysics and fluid mechanics. For example, large-scale Lagrangian (particle) tracking of bird-flocks (Attanasi et al. 2015) and super-large-scale particle image velocimetry using natural snowfall (Toloui et al. 2014). While large-scale laboratory experiments (Kuhn et al. 2010) allow efficient use of non-linear polynomial camera mappings (Soloff et al. 1997, Wieneke 2005 and 2008) their application at length-scales beyond laboratory practice is limited. Firstly, physical constraints limit the size for a calibration target allowing it to cover only a portion of the measurement domain. Secondly, accurate spatial positioning is hampered by limited access and absence of conventional laboratory equipment.

Here we combine methods developed in computer vision (Hartley and Zisserman, 2004) with non-linear polynomial camera mappings known from experimental fluid mechanics (Soloff et al. 1997). We extend the planar checkerboard calibration of Zhang (2000) to multiple views (Geiger et al. 2012) and correct for optical distortion by rectifying lines (Devernay and Faugeras, 2001). The method allows the planar calibration object to be much smaller than the measurement volume and is therefore versatile for spaces that are large and have limited access.

2. Experimental Setup and Calibration Procedure

Using a four camera system (LaVision 5.5M sCMOS) we image inside a large measurement volume of $\sim 10 \times 25 \times 6$ [m] at the large-scale ocean aquarium of the Rotterdam Zoo (see Fig. 1). A combination of wide-angle lenses (Nikkor AF 24 [mm]) and a large depth of field (~ 25 [m]) cause non-affine imaging conditions with significant magnification over the depth of field, while the difference in the refractive index between air and water contribute to optical distortion.

To calibrate the camera setup we use planar checkerboard target (Zhang, 2000) of 1.5×1.8 [m] with 5×6 tiles (Geiger et al. 2012) that is positioned under unknown position and orientation using a team of divers (see Fig. 1). Processing the camera calibration requires to first correct for optical distortion (Devernay and Faugeras, 2001), here rectifying curves obtained from the checkerboard images by minimizing the total relative curvature. Once dewarped we perform a single-view camera calibration for each camera where the checkerboard triangulation is used to find the unknown rotations and translations between the different views (Geiger et al. 2012). This allows us to define a unique camera calibration that can be further refined by optimizing the reprojection error (Hartley and Zisserman, 2004).

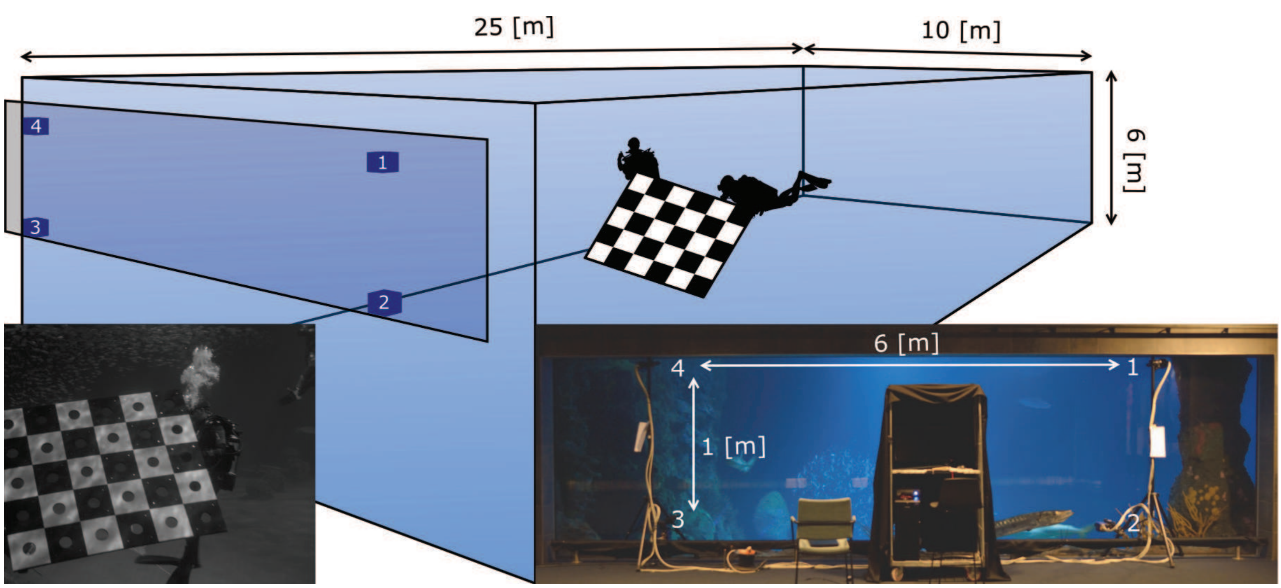

Fig. 1 Four-camera setup at the Rotterdam zoo including a schematic representation of the large measurement volume including imaging a planar checkerboard calibration target.

3. Results

The resulting camera calibration is shown in Fig. 2. including a brief summary of the results in Tab. 1. Firstly, a 3rd order distortion mapping significantly minimizes the total relative curvature $\bar{\kappa}$ to ~ 1 [%], indicating low optical distortion with respect to the checkerboard size in the dewarped image-plane. Secondly, we obtain low re-projection errors $\varepsilon \sim 1$ [px], which indicate spatial accuracy of ~ 1 [cm] over the entire measurement volume when rationalized with respect to the checkerboard target. At last, correcting for the difference in refractive index between air and water, the focal length from the camera calibration matrix lies close to the focal length of the lens, while the relative positioning reproduces the original camera positioning of the experiment setup in Fig. 1.

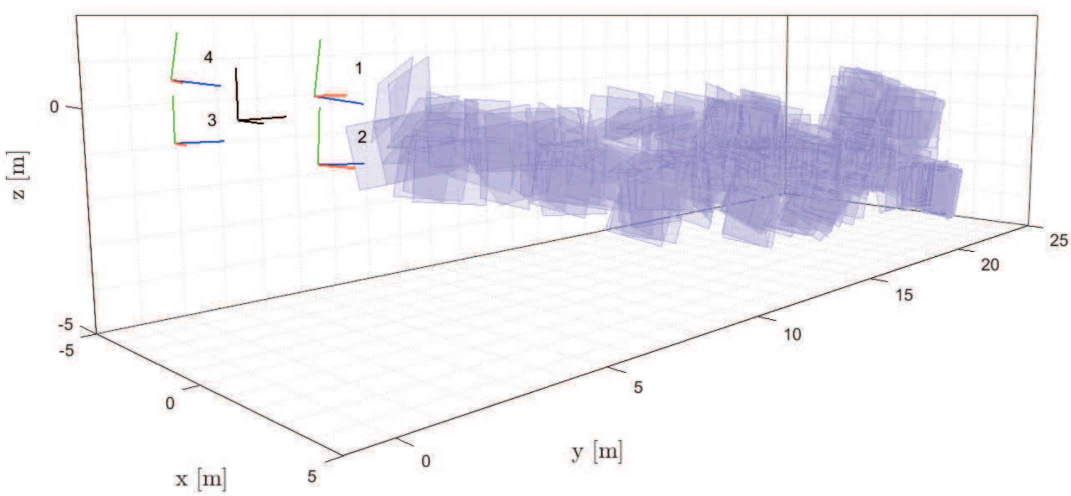

Fig. 2 The resulting camera calibration showing a reconstruction of the virtual-camera centers and orientations, including a triangulation ±175 checkerboards that sample the measurement volume.

	Camera 1	Camera 2	Camera 3	Camera 4
$\bar{\kappa}[-]$	$1.0 \pm 1.2\mathrm{e}-2$	$1.0 \pm 1.1\mathrm{e}-2$	$1.1 \pm 1.8\mathrm{e}-2$	$1.1 \pm 1.3\mathrm{e}-2$
$\varepsilon[px]$	2.07 ± 1.93	1.67 ± 1.51	1.77 ± 1.36	1.34 ± 1.02
$f[mm]$	24.4	23.6	26.1	26.0
$x[m]$	2.822	2.843	−2.817	−2.849
$y[m]$	−0.005	0.005	−0.005	0.005
$z[m]$	0.605	−0.599	−0.665	0.659

Tab. 1 Brief summary of the results from the obtained camera calibration. From top to bottom: the relative curvature, the reprojection error, the obtained focal length and the camera positioning.

3. Application to Field Experiments

Using the obtained camera calibration allows image processing in the dewarped image-plane and accurate three-dimensional measurement inside the large-scale ocean aquarium. To validate the accuracy of the camera calibration we feature-point-match the fin of a freely swimming shark. As can be seen in Fig. 3. we obtain an accurate ray tracing that consistently crosses the shark fin in the same location allowing to triangulate its position. This allows further application of tracking and tomographic methods, here down to a length-scale of 1 [cm] over large distance spanning several tens of meters.

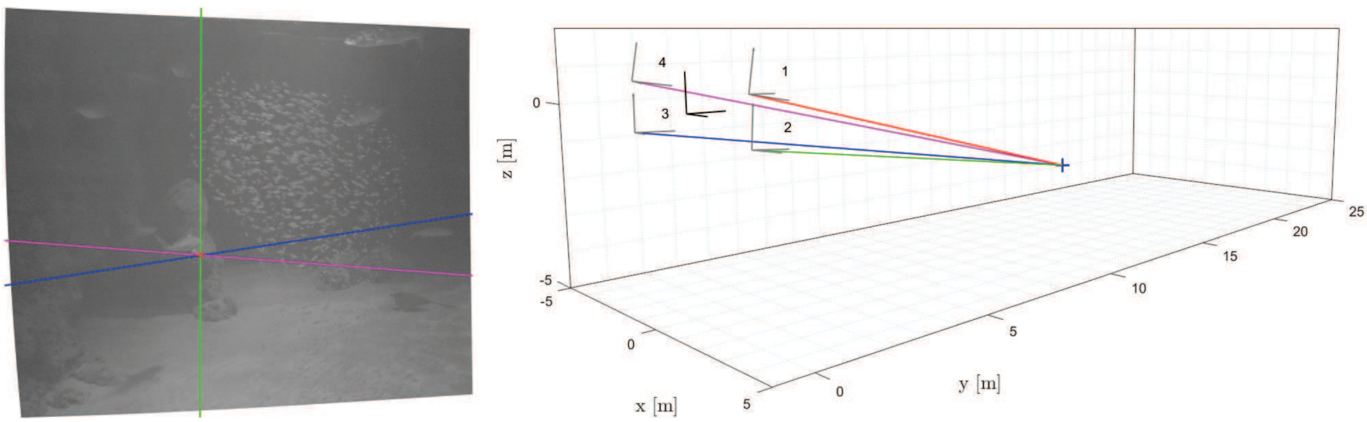

Fig. 3 Consistent ray tracing of the tip of a shark fin including a three dimensional triangulation.

4. Conclusion

Combining methods known from computer vision and non-linear camera mappings developed in experimental fluid mechanics we have successfully obtained a large-scale camera calibration in the order of tens of meters. Despite to the relative small size of the planar calibration object, a high accuracy has been obtained over the entire measurement volume. The method is versatile for spaces that have limited access and can be efficiently applied in absence of any laboratory equipment. The resulting calibration allows accurate imaging over a large measurement volume, here with application to biological fluid mechanics.

References

Attanasi A, Cavagna A, Del Castello L, Giardina I, Jelic A, Melillo S, Parisi L, Pellacini F, Shen E, Silvestri E, and Viale M (2015) Greta - A novel global and recursive tracking algorithm in three dimensions. IEEE Transactions on Pattern Analysis and Machine Intelligence, 37:2451-2463.

Geiger A, Moosmann F, Car O, and Schuster B (2012) Automatic camera and range sensor calibration using a single shot. IEEE International Conference on Robotics and Automation.

Hartley R I and Zisserman A (2004) Multiple View Geometry in Computer Vision. Cambridge University Press, Cambridge

Kuhn M, Ehrenfried K, Bosbach J, and Wagner C (2010) Large-scale tomographic particle image velocimetry using helium-filled soap bubbles. Experiments in Fluids, 50:929-948.

Soloff S M, Adrian R J, and Liu. Z-C (1997) Distortion compensation for generalized stereoscopic particle image velocimetry. Measurement Science and Technology, 8:1441-1454.

Toloui M, Riley S, Hong J, Howard K, Chamorro L P, Guala M, and Tucker J (2014) Measurement of atmospheric boundary layer based on super-large-scale particle image velocimetry using natural snowfall. Experiments in Fluids, 55: 1737.

Wieneke B (2005) Stereo-piv using self-calibration on particle images. Experiments in Fluids, 39:267-280.

Wieneke B (2008) Volume self-calibration for 3d particle image velocimetry. Experiments in Fluids, 45:549-556

Zhang Z (2000) A flexible new technique for camera calibration. IEEE Transactions on Pattern Analysis and Machine Intelligence, 22:1330-1334